Combined two-photon microscopy and angiographic optical coherence tomography

Bumju Kim
Tae Jun Wang
Qingyun Li
Jutaek Nam
Sekyu Hwang
Euiheon Chung
Sungjee Kim
Ki Hean Kim

Combined two-photon microscopy and angiographic optical coherence tomography

Bumju Kim,[a*] **Tae Jun Wang,**[b*] **Qingyun Li,**[a] **Jutaek Nam,**[c] **Sekyu Hwang,**[c] **Euiheon Chung,**[d] **Sungjee Kim,**[c] **and Ki Hean Kim**[a,b]

[a]Pohang University of Science and Technology, Department of Mechanical Engineering, San 31 Hyoja-dong, Nam-gu, Pohang, Gyeongbuk 790-784, Republic of Korea
[b]Pohang University of Science and Technology, Division of Integrative Biosciences and Biotechnology, San 31 Hyoja-dong, Nam-gu, Pohang, Gyeongbuk 790-784, Republic of Korea
[c]Pohang University of Science and Technology, Department of Chemistry, San 31 Hyoja-dong, Nam-gu, Pohang, Gyeongbuk 790-784, Republic of Korea
[d]Gwangju Institute of Science and Technology, School of Mechatronics, Department of Medical System Engineering, 123 Cheomdan-gwagiro, Buk-gu, Gwangju 500-712, Republic of Korea

Abstract. A combined two-photon microscopy (TPM) and angiographic optical coherence tomography (OCT) is developed, which can provide molecular, cellular, structural, and vascular information of tissue specimens *in vivo*. This combined system is implemented by adding an OCT vasculature visualization method to the previous combined TPM and OCT, and then is applied to *in vivo* tissue imaging. Two animal models, a mouse brain cranial window model and a mouse ear cancer model, are used. Both molecular, cellular information at local regions of tissues, and structural, vascular information at relatively larger regions are visualized in the same sections. *In vivo* tissue microenvironments are better elucidated by the combined TPM and angiographic OCT. © *The Authors. Published by SPIE under a Creative Commons Attribution 3.0 Unported License. Distribution or reproduction of this work in whole or in part requires full attribution of the original publication, including its DOI.* [DOI: 10.1117/1.JBO.18.8.080502]

1 Introduction

Both two-photon microscopy (TPM) and optical coherence tomography (OCT) are three-dimensional (3-D) tissue imaging techniques with high imaging depths. TPM is a 3-D microscopic technique based on two-photon excitation and other nonlinear processes, and provides molecular and cellular information of tissues at subcellular resolutions down to a few hundred micrometers deep from the surface.[1] OCT is another 3-D technique based on light back scattering, and provides structural information at <10 micrometer resolutions down to a few millimeters deep from the surface.[2] Since TPM and OCT are based on different contrast mechanisms, their combination is beneficial by providing complementary information. Various methods to combine TPM and OCT or optical coherence microscopy (OCM) have been developed.[3–5] One method was to use single Ti-sapphire lasers with a very short pulse width in the range of 10 fs, for a combined TPM and OCM.[3] This method was applied to miniaturized imaging probes with double clad fibers.[3,4] A method of combined TPM and OCT was developed by using two objective lenses of different magnifications for imaging at different length scales.[5] We recently developed a combined TPM and OCT by using separate light sources for optimal imaging conditions of individual modalities: a wavelength tunable Ti-sapphire laser and a wavelength-swept light source with its center wavelength of ~1310 nm for TPM and OCT, respectively.[6] Both TPM and OCT images were obtained with a single objective lens by controlling illumination or excitation beam sizes. Local cellular distribution within tissues and tissue structure in the surrounding regions were visualized in 3-D. Additional important information of *in vivo* tissues is vasculature. In tumor microenvironment, abnormal tumor vasculature is one of the hallmarks of cancer. Angiogenesis is required for the growth of tumor and provides route for cancer cell metastasis.[7] There are various OCT methods for vasculature visualization.

In this article, we developed a combined TPM and angiographic OCT in order to provide vascular information of tissues together with molecular, cellular, and structural information in the same tissue sections. Angiographic OCT was implemented by adapting one of OCT vasculature visualization methods. Combined TPM and angiographic OCT was applied to *in vivo* imaging of mouse models including a cancer model as demonstration.

2 Materials and Methods

2.1 Imaging System

Optical configuration of the combined TPM and angiographic OCT was based the previously combined system with some modifications.[6] In short, imaging beams from two separate light sources were combined by a dichroic mirror after separate scanners and scan lenses. Combined beams went through a tube lens and an objective lens and were focused at the sample. A water immersion objective lens (XLUMPlanFLN, Olympus 20X, 1.0 NA) was used, and different beam diameters were used for TPM and OCT. Fluorescent and reflected light from the sample was collected by the objective lens, split, and processed at separate detection setups. There were a few changes from the original setup. (1) A new OCT light source (SSOCT-1310, Axsun) was used. (2) NA for OCT was changed to 0.04 by using 1 mm beam diameter on the back aperture of objective lens. The depth of focus and transverse resolution were adjusted to 750 and 10 μm, respectively.

OCT methods for vasculature visualization can be categorized into Doppler-based methods[8–10] and temporal variation-based methods.[11–15] The former is based on the phase changes or frequency shift due to moving particles as Doppler effect.[8,9] While this method provides flow rate information within vasculature, there is inherent angular dependency in the measurement. Optical microangiography is another Doppler-based method

---
*These authors contributed equally to the paper.

Address all correspondence to: Ki Hean Kim, Pohang University of Science and Technology, Department of Mechanical Engineering, San 31 Hyoja-dong, Nam-gu, Pohang, Gyeongbuk 790-784, Republic of Korea. Tel: 82-54-279-2190; Fax: 82-54-279-3199; E-mail: kiheankim@postech.edu

that separates scattering signal caused by flow from static tissue background effectively by heterodyne technology.[10] The latter is based on temporal variation of phase or intensity due to the flow of particles. Both phase variance and intensity variance methods provide high-sensitive vasculature contrast.[11–15] In the current setup, angiographic imaging was implemented by adapting an intensity variance method.[15]

In TPM, x to y plane images were acquired with stepwise increment by 2 μm in the z direction from the surface. The field of view (FOV) was approximately 300×300 μm^2, and each image consisted of 512×512 pixels. Excitation wavelength was set at 780 nm for auto-fluorescence and at 930 nm for green fluorescent protein (GFP). The imaging time was approximately 2 to 8 min /volume. In OCT, multiple cross-sectional images in the x to z plane were acquired with stepwise increments in the y direction by 5 μm. Each cross-sectional image was composed of 300 depth-scans, and FOV was 980×980 μm^2 in the x to y plane. For angiographic imaging, five cross-sectional images were acquired at each y position to calculate intensity variance. The imaging time was approximately 10 s/volume. Spatial coregistration of TPM and OCT images was made by imaging a sample of fluorescent microspheres, which were 5 μm yellow-green and were embedded in 5% agarose, with both TPM and OCT. A transformation map was generated to overlap 3-D positions of the microspheres in two images.

2.2 Sample Preparation

Combined TPM and angiographic OCT was applied to *in vivo* imaging of two animal models: a mouse brain model and a mouse ear cancer model. The mouse brain model uses chronic cranial window model[16] with a GFP mouse [CByJ.B6-Tg(CAG-EGFP)10sb/J]. After the cranial window surgery, a circular ring was attached around the cranial window with dental cement. The mouse brain was held fixed with a custom-made ring holder during imaging. A mouse ear cancer model was made by injecting melanoma cells into the ears of nude mice superficially and by growing them for a few days. The mouse ear cancer model was held with an ear bar and the ear was attached onto the bar by using a double-sided tape. The animal was sedated by using isoflurane gas, and body temperature was maintained with a heating pad during imaging. Both nude mouse and GFP mouse models were obtained from the Jackson Laboratory, and bred at the animal facility of POSTECH Biotech Center under specific pathogen-free conditions.

3 Results

In vivo mouse brain images with the combined system were shown in Fig. 1. A projected angiographic OCT image in the x to y plane was in (a), and it showed dense vasculature in the brain. FOV of TPM image was marked as a rectangle in (a). A TPM image at 144 μm depth from the surface and its overlaid image with an angiographic OCT image were shown in (b) and (c), respectively. This overlaid angiographic OCT image was not a projection image but the one at a single depth range. TPM image showed neural cells and extracellular matrix (ECM) expressing GFP in the brain. Blood vessels appeared dark in the image due to absence of GFP. TPM image was coregistered well with the angiographic OCT image based on vascular structure. A mosaic image of 3×3 projected angiographic OCT images was shown in (d). Its size was 2×2 mm^2 with
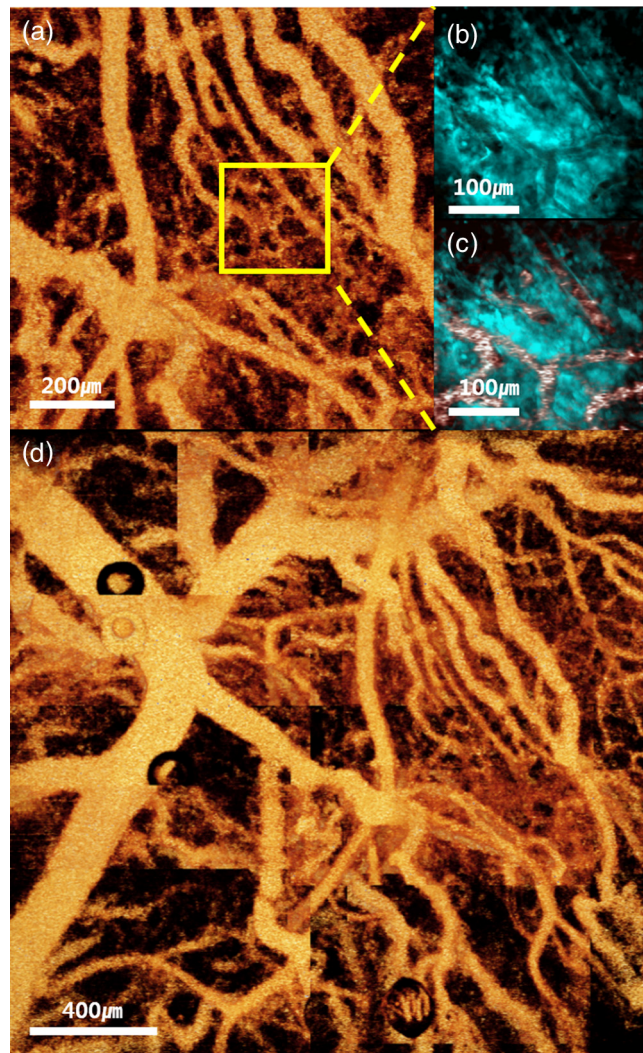

Fig. 1 (a) Two-photon microscopy (TPM) and angiographic optical coherence tomography (OCT) images of a mouse cranial window model. Angiographic OCT image, (b) TPM image (Video 1, MOV, 1.51 MB) [URL: http://dx.doi.org/10.1117/1.JBO.18.8.080502.1], (c) overlaid angiographic and TPM image in TPM field of view (FOV), and (d) large sectional angiographic OCT image. Black circular shapes in the images are air bubbles.

some overlap between images. Large-sectional vasculature distribution could be visualized.

The images of the mouse ear cancer model were shown in Fig. 2. Both the normal and cancer sections were shown in (a to c) and (d to f), respectively. In each section, an OCT cross-sectional intensity image in the x to z plane, an OCT angiographic image in the x to y plane, and a TPM image in the x to y plane were shown. TPM images were acquired based on intrinsic signal. OCT cross-sectional image of the normal section showed typical layered structures of mouse ear: superficial epidermis and dermis on both sides of the ear and cartilage in the middle as two lines in the image (a). The entire cross section of the mouse ear was shown, and its thickness was ~440 μm. Below the mouse ear, the top surface of a mouse ear holder was shown as an artifact. OCT angiographic image, which was generated by maximum intensity projection, showed vasculature of the mouse ear (b). OCT angiographic image shows regular smooth vascular distribution. A box in
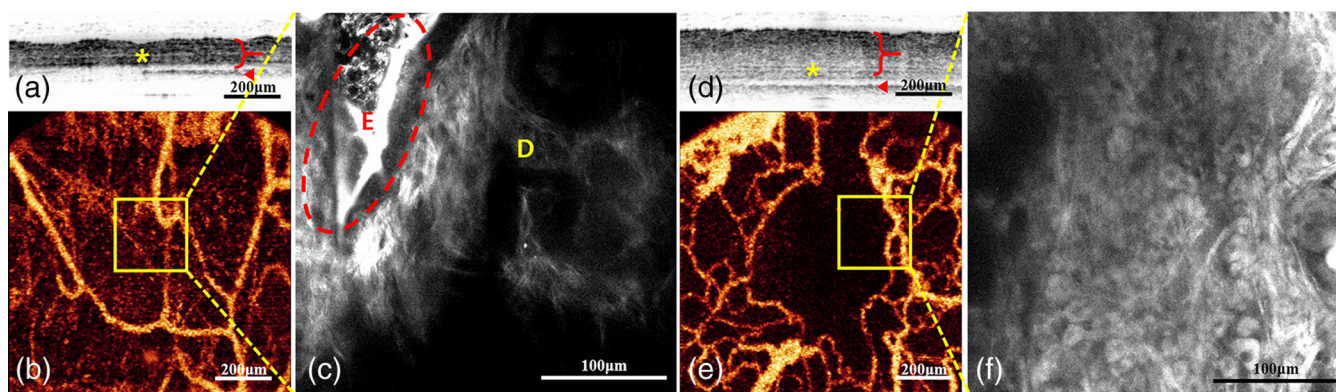
Fig. 2 Combined TPM and angiographic OCT image of a mouse ear cancer model. Normal and tumor sections are shown in (a–c) and (d–f), respectively. In each section, cross-sectional OCT intensity image (a, d), OCT angiographic image (b, e), and TPM images (c, f) are shown. (Video 2, MOV, 2.15 MB [URL: http://dx.doi.org/10.1117/1.JBO.18.8.080502.2]; Video 3, MOV, 3.18 MB [URL: http://dx.doi.org/10.1117/1.JBO.18.8.080502.3]). Brackets, stars, and arrow heads in (a) and (d) indicate whole thickness of the mouse ear, cartilage inside the mouse ear, and top surface of the mouse holder respectively. *E* and *D* in (c) indicated the epithelium and dermis respectively.

the angiographic OCT image indicates TPM FOV. Zoomed TPM image showed dermal layer at 68 μm depth (c). Mostly fibrous structures of ECM were shown, and there were some epidermis left in the image due to surface irregularity.

In the tumor section, the ear appeared thicker due to cancer cell mass in the cross-sectional image (d). Since the cartilage layer appeared close to the bottom surface, the cancer cells seemed to be located in the upper side of ear. OCT angiographic image showed that large blood vessels were mainly distributed in the periphery of the image, and this might be due to the cancer cell injection (e). TPM image in the tumor section shows some cells in the dermis, which might be injected cancer cells (f).

4 Discussion

To our knowledge, this is the first demonstration of visualizing both cancer cells distribution and surrounding vasculature within tissues *in vivo* based on different contrast mechanisms. Combined TPM and angiographic OCT could be useful for visualization of tumor microenvironment. OCT could be used to screen tumor sections rapidly and to identify regions of interest, and then TPM could be used to do high-resolution cellular, molecular imaging at those regions. Various *in vivo* studies can be performed by using the combined TPM and angiographic OCT, and examples are *in vivo* studies of tumor or immune response.

References

1. W. Denk, J. H. Strickler, and W. W. Webb, "Two-photon laser scanning fluorescence microscopy," *Science* **248**(4951), 73–76 (1990).
2. D. Huang et al., "Optical coherence tomography," *Science* **254**(5035), 1178–1181 (1991).
3. G. Liu and Z. Chen, "Fiber-based combined optical coherence and multiphoton endomicroscopy," *J. Biomed. Opt.* **16**(3), 036010 (2011).
4. J. Xi et al., "Integrated multimodal endomicroscopy platform for simultaneous en face optical coherence and two-photon fluorescence imaging," *Opt. Lett.* **37**(3), 362–364 (2012).
5. S. Tang et al., "Multiscale multimodal imaging with multiphoton microscopy and optical coherence tomography," *Opt. Lett.* **36**(24), 4800–4802 (2011).
6. B. Jeong et al., "Combined two-photon microscopy and optical coherence tomography using individually optimized sources," *Opt. Express* **19**(14), 13089–13096 (2011).
7. P. Carmeliet and R. K. Jain, "Molecular mechanisms and clinical applications of angiogenesis," *Nature* **473**(7347), 298–307 (2011).
8. S. Yazdanfar, M. Kulkarni, and J. Izatt, "High resolution imaging of in vivo cardiac dynamics using color Doppler optical coherence tomography," *Opt. Express* **1**(13), 424–431 (1997).
9. S. Makita et al., "Comprehensive in vivo micro-vascular imaging of the human eye by dual-beam-scan Doppler optical coherence angiography," *Opt. Express* **19**(2), 1271–1283 (2011).
10. R. K. Wang et al., "Three dimensional optical angiography," *Opt. Express* **15**(7), 4083–4097 (2007).
11. B. J. Vakoc et al., "Three-dimensional microscopy of the tumor microenvironment in vivo using optical frequency domain imaging," *Nat. Med.* **15**(10), 1219–1223 (2009).
12. Y. Zhao et al., "Doppler standard deviation imaging for clinical monitoring of in vivo human skin blood flow," *Opt. Lett.* **25**(18), 1358–1360 (2000).
13. J. Fingler et al., "Mobility and transverse flow visualization using phase variance contrast with spectral domain optical coherence tomography," *Opt. Express* **15**(20), 12636–12653 (2007).
14. X. Liu et al., "Spectroscopic-speckle variance OCT for microvasculature detection and analysis," *Biomed. Opt. Express* **2**(11), 2995–3009 (2011).
15. A. Mariampillai et al., "Speckle variance detection of microvasculature using swept-source optical coherence tomography," *Opt. Lett.* **33**(13), 1530–1532 (2008).
16. N. D. Kirpatrick et al., "Video-rate resonant scanning multiphoton microscopy: An emerging technique for intravital imaging of the tumor microenvironment," *IntraVital* **1**(1), 60–68 (2012).